

A Cut Finite Element Method for a Model of Pressure in Fractured Media

Erik Burman^{*}, Peter Hansbo[†], and Mats G. Larson[‡]

^{*}*Department of Mathematics, University College London, London, UK-WC1E 6BT, United Kingdom*

[†]*Department of Mechanical Engineering, Jönköping University, SE-55111 Jönköping, Sweden*

[‡]*Department of Mathematics and Mathematical Statistics, Umeå University, SE-901 87 Umeå, Sweden*

Abstract

We develop a robust cut finite element method for a model of diffusion in fractured media consisting of a bulk domain with embedded cracks. The crack has its own pressure field and can cut through the bulk mesh in a very general fashion. Starting from a common background bulk mesh, that covers the domain, finite element spaces are constructed for the interface and bulk subdomains leading to efficient computations of the coupling terms. The crack pressure field also uses the bulk mesh for its representation. The interface conditions are a generalized form of conditions of Robin type previously considered in the literature which allows the modeling of a range of flow regimes across the fracture. The method is robust in the following way: 1. Stability of the formulation in the full range of parameter choices; and 2. Not sensitive to the location of the interface in the background mesh. We derive an optimal order a priori error estimate and present illustrating numerical examples.

1 Introduction

The numerical modelling of flow in fractured porous media is important both in environmental science and in industrial applications. It is therefore not surprising that it is currently receiving increasing attention from the scientific computing community. Here we are interested in models where the fractures are modelled as embedded surfaces of dimension $d - 1$ in a d dimensional bulk domain. Models on this type of geometries of mixed dimension are typically obtained by averaging the flow equations across the width of the fracture and introducing suitable coupling conditions for the modelling of the interaction with the bulk flow. Such reduced models have been derived for instance in [20, 24, 1]. The coupling conditions in these models typically take the form of

a Robin type condition. The physical properties of the coupling enters as parameters in this interface condition. The size of these parameters can vary with several orders of magnitude depending on the physical properties of the crack and of the material in the porous matrix. This makes it challenging to derive methods that both are flexible with respect to mesh geometries and robust with respect to coupling conditions. A wide variety of different strategies for the discretisation of fractured porous media flow has been proposed in the literature. One approach is to use a method that allows for nonconforming coupling between the bulk mesh and the fracture mesh [3], or even arbitrary polyhedral elements in the bulk mesh in order to be able to mesh the fractures easily. This latter approach has been developed using discontinuous Galerkin methods [2], virtual element methods [15] and high order hybridised methods [13].

Herein we will consider an unfitted approach, drawing on previous work [4, 12, 10] where flow in fractured porous media was modelled in the situation where the pressure is a globally continuous function. When using unfitted finite element methods, the bulk mesh can be created completely independently of the fractures. Instead the finite element space is modified locally to allow for discontinuities across fractures and interface conditions are typically imposed weakly, or using methods similar to Nitsche's method. For other recent work using unfitted methods we refer to [22], where a stabilized Lagrange multiplier method is considered for the interface coupling and [14] where a mixed method is considered for the Darcy's equations both in the bulk and on the surface.

The upshot here, compared to [10] is that the pressure in the crack has its own pressure, allowing for the accurate approximation of problems where the pressure is discontinuous between the bulk and the fracture, and that the interface conditions are imposed in a way allowing for the full range of parameter values in the Robin condition, without loss of stability. We use the variant of the interface modelling considered in [24], that was also recently applied for the numerical modelling in [2]. In these models we may obtain a wide range of parameter values in the interface condition and we therefore develop a method which handle the full range of values and produces approximations with optimal order convergence. The approach is inspired by the work of Stenberg [21] and may be viewed as a version of the Nitsche method that can handle Robin type conditions and which converges to the standard Nitsche method when the Robin parameter tends to infinity. Previous applications of this approach in the context of fitted finite elements include [18] and [28].

The finite element spaces are constructed starting from a standard mesh equipped with a finite element space. For each geometric domain (subdomains and interface) we mark all the elements intersected by the domain and then we restrict the finite element space to that set to form a finite element space for each domain. This procedure leads to cut finite elements and we use stabilization to ensure that the resulting form associated with the method is coercive and that the stiffness matrix is well conditioned. The stabilization is of face or ghost penalty type [5, 6, 23], and is added both to the bulk and interface spaces. Previous related work on cut finite element methods include the interface problem [17]; overlapping meshes [19]; coupled bulk-surface problems [11, 7,

10] and [16]; mixed dimensional problems [8], and surface partial differential equations [6, 25]. For a general introduction to cut finite element methods we refer to [4].

The outline of the paper is as follows: In Section 2 we introduce the model problem and discuss the relation between our formulation of the interface conditions and previous work; in Section 3 we formulate the cut finite element method; in Section 4 we prove the basic properties of the formulation and in particular an optimal order a priori error estimate which is uniform in the full range of interface parameters; and in Section 5 we present numerical results.

2 The Model Problem

2.1 Governing Equations

Let Ω be a convex polygonal domain in \mathbb{R}^d , $d = 2$ or 3 , with boundary $\partial\Omega$ and exterior unit normal n . Let Γ be a smooth embedded interface in Ω , which partitions Ω into two subdomains Ω_1 and Ω_2 with exterior unit normals n_1 and n_2 . We assume that Γ is a closed surface without boundary residing in the interior of Ω , more precisely we assume that there is $\delta_0 > 0$ such that the distance between Γ and $\partial\Omega$ is larger than δ . We consider for simplicity the case with homogeneous Dirichlet conditions on $\partial\Omega$.

The problem takes the form: find $u_i : \Omega_i \rightarrow \mathbb{R}$ and $u_\Gamma : \Gamma \rightarrow \mathbb{R}$ such that

$$-\nabla \cdot A_i \nabla u_i = f_i \quad \text{in } \Omega_i \quad (2.1)$$

$$-\nabla_\Gamma \cdot A_\Gamma \nabla_\Gamma u_\Gamma = f_\Gamma + \llbracket n \cdot A \nabla u \rrbracket \quad \text{on } \Gamma \quad (2.2)$$

$$n \cdot A \nabla u + B(u - u_\Gamma) = 0 \quad \text{on } \Gamma \quad (2.3)$$

$$u = 0 \quad \text{on } \partial\Omega \quad (2.4)$$

Here the jump (or sum) of the normal fluxes is defined by

$$\llbracket n \cdot A \nabla v \rrbracket = \sum_{i=1}^2 n_i \cdot A_i \nabla v_i, \quad (2.5)$$

In the interface condition (2.3), B is a 2×2 symmetric matrix with eigenvalues λ_i such that $\lambda_i \in [0, \infty)$ and we used the notation

$$n \cdot A \nabla v = \begin{bmatrix} n_1 \cdot A_1 \nabla v_1 \\ n_2 \cdot A_2 \nabla v_2 \end{bmatrix}, \quad v - v_\Gamma = \begin{bmatrix} v_1 - v_\Gamma \\ v_2 - v_\Gamma \end{bmatrix} \quad (2.6)$$

and thus in component form (2.3) reads

$$\begin{bmatrix} n_1 \cdot A_1 \nabla u_1 \\ n_2 \cdot A_2 \nabla u_2 \end{bmatrix} + B \begin{bmatrix} u_1 - u_\Gamma \\ u_2 - u_\Gamma \end{bmatrix} = \begin{bmatrix} 0 \\ 0 \end{bmatrix} \quad (2.7)$$

The coefficients A_1 , A_2 , are smooth uniformly positive definite symmetric $d \times d$ matrices, A_Γ is smooth tangential to Γ and uniformly positive definite on the

tangent space of Γ , so that

$$\sum_{i=1}^2 \|\nabla v_i\|_{\Omega_i}^2 + \|\nabla_\Gamma v_\Gamma\|_\Gamma^2 \lesssim \sum_{i=1}^2 (A_i \nabla v_i, \nabla v_i)_{\Omega_i} + (A_\Gamma \nabla_\Gamma v_\Gamma, \nabla_\Gamma v_\Gamma) \quad (2.8)$$

where \lesssim denotes less or equal up to a constant. Finally we assume $f_i \in L_2(\Omega_i)$ and $f_\Gamma \in L_2(\Gamma)$.

Remark 2.1 Several generalizations are possible on the external boundary. For instance, we may let the interface intersect the boundary of Ω . In this case we let ν denote the unit exterior conormal to $\Gamma \cap \partial\Omega$, i.e. ν is tangent to Γ and normal to $\partial\Omega \cap \Gamma$, and we assume that $\nu \cdot n \geq c > 0$ for some constant c so that the interface is transversal to $\partial\Omega$. We may then enforce the Dirichlet condition $u_\Gamma = g_\Gamma$ on $\partial\Omega \cap \Gamma$ (see [9]) or some other standard boundary condition.

Remark 2.2 In practical modeling we may want to take the thickness of the interface into account. Assuming that the permeability matrix in an interface of thickness t takes the form

$$A|_{U_{t/2}(\Gamma)} = A_\Gamma^e + a_\Gamma^e n_\Gamma \otimes n_\Gamma \quad (2.9)$$

where n_Γ is a unit normal vector field to Γ , $U_{t/2}(\Gamma)$ is the set of points with distance less than $t/2$ to Γ , v^e denotes the extension of a function v on Γ that is constant in the normal direction, A_Γ is the tangential tangential permeability tensor, and finally $a_{\Gamma,n}$ is the permeability across the interface. Also assuming that $f = f_\Gamma^e$ and $u = u^e$ in $U_{t/2}(\Gamma)$, the equation on the interface (2.2) may be modelled as follows

$$-\nabla_\Gamma \cdot t A_\Gamma \nabla_\Gamma u_\Gamma = t f_\Gamma + \llbracket n \cdot A \nabla u \rrbracket \quad \text{on } \Gamma \quad (2.10)$$

Note that the last term on the right hand side does not scale with t since it accounts for flow into the crack from the bulk domains.

Remark 2.3 We comment on how our interface condition (2.3) relates to the condition in [24] and later reformulated, see [2], in terms of averages and jumps of the bulk fields across the interface. The interface conditions in [24], equations (3.18) and (3.19), takes the form

$$\xi n_1 \cdot A_1 \nabla v_1 - (1 - \xi) n_2 \cdot A_2 \nabla v_2 = \alpha (v_\Gamma - v_1) \quad (2.11)$$

$$\xi n_2 \cdot A_2 \nabla v_2 - (1 - \xi) n_1 \cdot A_1 \nabla v_1 = \alpha (v_\Gamma - v_2) \quad (2.12)$$

where ξ and α are parameters. The parameter α is related to physical properties of the interface as follows

$$\alpha = \frac{2a_{\Gamma,n}}{d} \quad (2.13)$$

where $a_{\Gamma,n}$ is the permeability coefficient across the interface Γ and d is the thickness of the interface, see (3.8) in [24]. In matrix form we obtain

$$\begin{bmatrix} \xi & \xi - 1 \\ \xi - 1 & \xi \end{bmatrix} \begin{bmatrix} n_1 \cdot A_1 \nabla v_1 \\ n_2 \cdot A_2 \nabla v_2 \end{bmatrix} + \begin{bmatrix} \alpha & 0 \\ 0 & \alpha \end{bmatrix} \begin{bmatrix} v_1 - v_\Gamma \\ v_2 - v_\Gamma \end{bmatrix} = 0 \quad (2.14)$$

which leads to

$$B = \frac{1}{2\xi - 1} \begin{bmatrix} \xi & 1 - \xi \\ 1 - \xi & \xi \end{bmatrix} \begin{bmatrix} \alpha & 0 \\ 0 & \alpha \end{bmatrix} = \frac{\alpha}{2\xi - 1} \begin{bmatrix} \xi & 1 - \xi \\ 1 - \xi & \xi \end{bmatrix} \quad (2.15)$$

We note that we have the eigen pairs

$$Be_1 = \underbrace{\frac{\alpha}{2\xi - 1}}_{\lambda_1} e_1, \quad Be_2 = \underbrace{\alpha}_{\lambda_2} e_2 \quad (2.16)$$

with the corresponding eigen vectors defined by

$$e_1 = \frac{1}{\sqrt{2}} \begin{bmatrix} 1 \\ 1 \end{bmatrix} \quad \text{and} \quad e_2 = \frac{1}{\sqrt{2}} \begin{bmatrix} 1 \\ -1 \end{bmatrix}$$

and thus B is positive definite for $\xi > 1/2$, singular for $\xi = 1/2$, and indefinite for $\xi < 1/2$. It is therefore natural to consider the case when $\alpha > 0$ and $\xi > 1/2$. We remark that when α tends to infinity both eigenvalues tend to infinity and when ξ tends to $1/2$ from above one eigenvalue tends to infinity. It is therefore important to construct a method which is robust in the full range $\lambda_i \in (0, \infty)$ of possible values for the two eigenvalues

To see the relation to the formulation of the interface conditions in [2] we first note that we have the expansions

$$\begin{bmatrix} n_1 \cdot A_1 \nabla v_1 \\ n_2 \cdot A_2 \nabla v_2 \end{bmatrix} = 2^{-1/2} \llbracket n \cdot A \nabla \rrbracket e_1 + 2^{1/2} \langle\langle n \cdot A \nabla v \rangle\rangle e_2 \quad (2.17)$$

$$\begin{bmatrix} v_1 - v_\Gamma \\ v_2 - v_\Gamma \end{bmatrix} = 2^{1/2} (\langle\langle v \rangle\rangle - v_\Gamma) e_1 + 2^{-1/2} \llbracket v \rrbracket e_2 \quad (2.18)$$

where the jumps and averages of the bulk fields across the the interface are defined by

$$\llbracket n \cdot A \nabla v \rrbracket = \sum_{i=1}^2 n_i \cdot A_i \nabla v_i, \quad \llbracket v \rrbracket = v_1 - v_2 \quad (2.19)$$

$$\langle\langle n \cdot A \nabla v \rangle\rangle = \frac{1}{2} (n_1 \cdot A_1 \nabla v_1 - n_2 \cdot A_2 \nabla v_2), \quad \langle\langle v \rangle\rangle = \frac{1}{2} (v_1 + v_2) \quad (2.20)$$

Using the expansions (2.17) and (2.18) together with (2.16) and matching the coefficients associated with each eigenvector we obtain the interface conditions

$$\llbracket n \cdot A \nabla v \rrbracket + \frac{2\alpha}{2\xi - 1} (\langle\langle v \rangle\rangle - v_\Gamma) = 0 \quad (2.21)$$

$$\langle\langle n \cdot A \nabla v \rangle\rangle + \frac{\alpha}{2} \llbracket v \rrbracket = 0 \quad (2.22)$$

which are precisely the conditions used in [2].

2.2 Weak Form

Define the function spaces

$$V = V_1 \oplus V_2 \oplus V_\Gamma \quad (2.23)$$

$$V_i = \{v_i \in H^1(\Omega_i) : v = 0 \text{ on } \partial\Omega \cap \partial\Omega_i\} \quad i = 1, 2 \quad (2.24)$$

$$V_\Gamma = \{v_\Gamma \in H^1(\Gamma) : v = 0 \text{ on } \partial\Omega \cap \Gamma\} \quad (2.25)$$

and let $v \in V$ denote the vector $v = (v_1, v_2, v_\Gamma)$. We will also use the notation \tilde{V} for functions $v \in V$ such that $v_i \in H^{\frac{3}{2}+\epsilon}(\Omega_i)$, $i = 1, 2$, and $v_\Gamma \in H^{\frac{3}{2}+\epsilon}(\Gamma)$, with $\epsilon > 0$. Using partial integration on Ω_i we obtain

$$\begin{aligned} \sum_{i=1}^2 (f_i, v_i)_{\Omega_i} &= \sum_{i=1}^2 (-\nabla \cdot A_i \nabla u_i, v_i)_{\Omega_i} \\ &= \sum_{i=1}^2 (A_i \nabla u_i, \nabla v_i)_{\Omega_i} - (n_i \cdot A_i \nabla u_i, v_i)_{\partial\Omega_i} \\ &= \sum_{i=1}^2 (A_i \nabla u_i, \nabla v_i)_{\Omega_i} - (n_i \cdot A_i \nabla u_i, v_i - v_\Gamma)_{\partial\Omega_i} - (n_i \cdot A_i \nabla u_i, v_\Gamma)_{\partial\Omega_i} \\ &= \sum_{i=1}^2 (A_i \nabla u_i, \nabla v_i)_{\Omega_i} - (n \cdot A \nabla u, v - v_\Gamma)_\Gamma - ([n \cdot A \nabla u], v_\Gamma)_\Gamma \\ &= \sum_{i=1}^2 (A_i \nabla u_i, \nabla v_i)_{\Omega_i} + (B(u - u_\Gamma), v - v_\Gamma)_\Gamma \\ &\quad + (A_\Gamma \nabla_\Gamma u_\Gamma, \nabla_\Gamma v_\Gamma)_\Gamma - (f_\Gamma, v_\Gamma)_\Gamma \end{aligned}$$

Thus we arrive at the weak problem: find $u = (u_1, u_2, u_\Gamma) \in V$ such that

$$\boxed{\mathcal{A}(u, v) = L(v) \quad \forall v \in V} \quad (2.26)$$

where the forms are defined by

$$\mathcal{A}(u, v) = \sum_{i=1}^2 (A_i \nabla u_i, \nabla v_i)_{\Omega_i} + (A_\Gamma \nabla_\Gamma u_\Gamma, \nabla_\Gamma v_\Gamma)_\Gamma + (B(u - u_\Gamma), v - v_\Gamma)_\Gamma \quad (2.27)$$

$$L(v) = \sum_{i=1}^2 (f_i, v_i)_{\Omega_i} + (f_\Gamma, v_\Gamma)_\Gamma \quad (2.28)$$

2.3 Existence and Uniqueness

Introducing the energy norm

$$\|v\|^2 = \sum_{i=1}^2 \|v\|_{H^1(\Omega_i)}^2 + \|v_\Gamma\|_{H^1(\Gamma)}^2 + \|v - v_\Gamma\|_\Gamma^2 \quad (2.29)$$

on V , we directly find using a Poincaré inequality and the Cauchy-Schwarz inequality that the form A is coercive and continuous

$$\|v\|^2 \lesssim \mathcal{A}(v, v), \quad \mathcal{A}(v, w) \lesssim \|v\| \|w\| \quad (2.30)$$

Furthermore, L is a continuous functional on V and it follows from the Lax-Milgram Lemma that there is a unique solution in V to (2.26).

In the case considered here where Γ is a smooth, closed interface the model problem (2.26) satisfies the elliptic regularity estimate

$$\|u_1\|_{H^2(\Omega_1)} + \|u_2\|_{H^2(\Omega_2)} + \|u_\Gamma\|_{H^2(\Gamma)} \lesssim \|f_1\|_{\Omega_1} + \|f_2\|_{\Omega_2} + \|f_\Gamma\|_\Gamma \quad (2.31)$$

This follows in a straightforward manner from standard regularity theory. First note that since $u_i \in H^1(\Omega_i)$, $i = 1, 2$, and $u_\Gamma \in H^1(\Gamma)$ we have $B(u - u_\Gamma)|_\Gamma \in [H^{\frac{1}{2}}(\Gamma)]^2$ and using (2.3), $n \cdot A \nabla u \in [H^{\frac{1}{2}}(\Gamma)]^2$. This means that the right hand side of (2.2) is in L^2 and hence $u_\Gamma \in H^2(\Gamma)$ by elliptic regularity. Considering once again (2.3) we see that in each subdomain the solution coincides with a single domain solution with a Robin condition with data in $H^{\frac{1}{2}}(\Gamma)$ on Γ . By the elliptic regularity of the Robin problem we can then conclude that (2.31) holds.

3 A Robust Finite Element Method

3.1 The Mesh and Finite Element Spaces

To formulate the finite element method we introduce the following notation:

- Let $\mathcal{T}_{h,0}$ be a quasiuniform mesh on Ω with mesh parameter $h \in (0, h_0]$. Define the active meshes

$$\mathcal{T}_{h,i} = \{T \in \mathcal{T}_{h,0} : T \cap \Omega_i \neq \emptyset\} \quad i = 1, 2, \quad \mathcal{T}_{h,\Gamma} = \{T \in \mathcal{T}_{h,0} : T \cap \Gamma \neq \emptyset\} \quad (3.1)$$

associated with the bulk domains Ω_i , $i = 1, 2$, and interface Γ , and the domains covered by the meshes

$$O_{h,i} = \cup_{T \in \mathcal{T}_{h,i}} T \quad i = 1, 2, \quad O_{h,\Gamma} = \cup_{T \in \mathcal{T}_{h,\Gamma}} T \quad (3.2)$$

- Let $\mathcal{T}_{h,i}(\Gamma) = \{T \in \mathcal{T}_{h,i} : T \cap \Gamma \neq \emptyset\}$ and define $\mathcal{F}_{h,i}$ as the set of all interior faces associated with an element in $\mathcal{T}_{h,i}(\partial\Omega_i)$.
- Let $\mathcal{F}_{h,\Gamma}$ be the set of all interior faces in $\mathcal{T}_{h,\Gamma}$ and $\mathcal{K}_{h,\Gamma} = \{K = T \cap \Gamma : T \in \mathcal{T}_{h,\Gamma}\}$.
- Let $V_{h,0}$ be the space of continuous piecewise linear functions on $\mathcal{T}_{h,0}$ and define

$$V_{h,i} = V_{h,0}|_{\mathcal{T}_{h,i}} \quad i = 1, 2, \quad V_{h,\Gamma} = V_{h,0}|_{\mathcal{T}_{h,\Gamma}} \quad (3.3)$$

and

$$V_h = V_{h,1} \oplus V_{h,2} \oplus V_{h,\Gamma} \quad (3.4)$$

3.2 Standard Formulation

The standard finite element method takes the form: find $u_h = (u_{h,1}, u_{h,2}, u_{h,\Gamma}) \in V_h = V_{h,1} \oplus V_{h,2} \oplus V_{h,\Gamma}$ such that

$$\mathcal{A}_h^S(u_h, v) = L(v) \quad \forall v \in V_h \quad (3.5)$$

Here the form \mathcal{A}_h^S is defined by

$$\mathcal{A}_h^S = \mathcal{A} + s_h \quad (3.6)$$

where s_h is a stabilization term of the form

$$s_h = s_{h,1} + s_{h,2} + s_{h,\Gamma} \quad (3.7)$$

with

$$s_{h,i}(v, w) = \sum_{F \in \mathcal{F}_{h,i}} h_F \|\zeta(A_i)\|_{\infty, F} (\llbracket n \cdot \nabla v \rrbracket, \llbracket n \nabla w \rrbracket)_F, \quad i = 1, 2$$

where $\zeta(X)$ denotes the maximum eigenvalue of the matrix X ,

$$\begin{aligned} s_{h,\Gamma}(v, w) &= \sum_{F \in \mathcal{F}_{h,\Gamma}} h_F \|\zeta(A_\Gamma)\|_{\infty, F \cap \Gamma} (\llbracket n \cdot \nabla v \rrbracket, \llbracket n \nabla w \rrbracket)_{\mathcal{F}_{h,\Gamma}} \\ &\quad + \sum_{T \in \mathcal{T}_{h,\Gamma}} h_K^2 \|\zeta(A_\Gamma)\|_{\infty, K \cap \Gamma} (n_\Gamma \cdot \nabla v, n_\Gamma \cdot \nabla w)_{T \cap \Gamma}. \end{aligned}$$

3.2.1 Properties of the Stabilization Terms

The rationale for the design of the stabilizing terms is that they improve the stability, while remaining consistent for sufficiently smooth solutions.

Accuracy relies on the following consistency property that is immediate from the definitions above. For any function $v \in H^{\frac{3}{2}+\epsilon}(O_{h,i})$ there holds $s_{h,i}(v, w) = 0$ for all $w \in V_{h,i} + H^{\frac{3}{2}+\epsilon}(O_{h,i})$, $i = 1, 2$. For any function $v \in H^{\frac{3}{2}+\epsilon}(O_{h,\Gamma})$, such that $n_\Gamma \cdot \nabla v = 0$ on Γ there holds $s_{h,\Gamma}(v, w) = 0$ for all $w \in V_{h,\Gamma} + H^{\frac{3}{2}+\epsilon}(O_{h,\Gamma})$.

The stability properties are well known and we collect them in the following Lemma.

Lemma 3.1 *There are constants such that*

$$\|\nabla v\|_{A_i, O_{h,i}}^2 \lesssim \|\nabla v\|_{A_i, \Omega_i}^2 + \|v\|_{s_{h,i}}^2 \quad i = 1, 2 \quad (3.8)$$

and

$$\|\nabla_\Gamma v\|_{A_\Gamma, O_{h,\Gamma}}^2 \lesssim \|\nabla_\Gamma v\|_{A_\Gamma, \Gamma}^2 + \|v\|_{s_{h,\Gamma}}^2 \quad (3.9)$$

where we introduced the (semi) norm $\|v\|_{s_h}^2 = s_h(v, v)$.

Proof. See [5], [6], and [23], with minor modifications to account for the varying coefficients. \square

Remark 3.1 *Observe that the hidden constants in Lemma 3.1 depend on the variation of the A_i and A_Γ .*

3.3 Robust Formulation

The stabilizing terms ensure robustness irrespective of the intersection of the fracture and the mesh. They do not counter instabilities due to degenerate B . Our aim is to design a formulation which is robust in the case when the eigenvalues of B degenerate. Indeed as we saw above as ξ approaches $1/2$, λ_1 blows up. For clarity we recall the abstract boundary condition

$$n \cdot A \nabla v + B(v - v_\Gamma) = 0 \quad (3.10)$$

where we now assume that the matrix B is a positive definite symmetric 2×2 matrix with eigenvalues λ_i and eigenvectors e_i , such that $\lambda_i \in (0, \infty)$ and thus one or both eigenvalues may become very large or small. To handle this situation we instead enforce

$$B^{-1}n \cdot A \nabla v + (v - v_\Gamma) = 0 \quad (3.11)$$

weakly using a modified Nitsche method. This approach was originally developed in [21] where fitted finite element approximation of Robin conditions were considered.

Derivation of an Alternative Weak Form. As before we have the identity

$$L(v) = \underbrace{\sum_{i=1}^2 (A_i \nabla u_i, \nabla v_i)_{\Omega_i} + (A_\Gamma \nabla_\Gamma u_\Gamma, \nabla_\Gamma v_\Gamma)_\Gamma - (n \cdot A \nabla u, v - v_\Gamma)_\Gamma}_{=: \mathcal{A}_1(u, v)} \quad (3.12)$$

$$= \mathcal{A}_1(u, v) - (n \cdot A \nabla u, v - v_\Gamma)_\Gamma \quad (3.13)$$

where we introduced the bilinear form \mathcal{A}_1 for brevity. To enforce the interface conditions we proceed as follows

$$\begin{aligned} L(v) &= \mathcal{A}_1(u, v) - (n \cdot A \nabla u, v - v_\Gamma)_\Gamma \\ &= \mathcal{A}_1(u, v) + (n \cdot A \nabla u, B^{-1}(n \cdot A \nabla v))_\Gamma \\ &\quad - (n \cdot A \nabla u, B^{-1}(n \cdot A \nabla v) + (v - v_\Gamma))_\Gamma \\ &= \mathcal{A}_1(u, v) + (n \cdot A \nabla u, B^{-1}(n \cdot A \nabla v))_\Gamma \\ &\quad - (n \cdot A \nabla u, B^{-1}(n \cdot A \nabla v) + (v - v_\Gamma))_\Gamma \\ &\quad - (B^{-1}(n \cdot A \nabla u) + (u - u_\Gamma), n \cdot A \nabla v)_\Gamma \\ &\quad + (B^{-1}(n \cdot A \nabla u) + (u - u_\Gamma), \tau(B^{-1}(n \cdot A \nabla v) + (v - v_\Gamma)))_\Gamma \end{aligned}$$

where the last two terms are zero due to the interface condition and the resulting form on the right hand side is symmetric. Furthermore, τ is a stabilization parameter (a 2×2 matrix) of the form

$$\tau = \sum_{i=1}^2 \tau_i e_i \otimes e_i, \quad \tau_i = \frac{\lambda_i \beta}{\lambda_i h + \beta} \quad i = 1, 2 \quad (3.14)$$

where β is a positive parameter and we recall that λ_i and e_i are the eigenvalues and eigenvectors of B . The parameter β is chosen so that

$$\|n\|_{A,\infty,\Gamma}^2 := \sum_{i=1}^2 \|n_i\|_{A_i,\infty,\Gamma}^2 \lesssim \beta \quad (3.15)$$

where $\|w\|_{A_i,\infty,\Gamma} := \|A_i^{\frac{1}{2}} w\|_{\infty,\omega}$ is the A_i weighted L^∞ norm over Γ .

Remark 3.2 *The choice of τ_i can be further refined as follows*

$$\tau_i = \frac{\lambda_i \beta_i}{\lambda_i h + \beta_i} \quad i = 1, 2 \quad (3.16)$$

with

$$\sum_{j=1}^2 \|n_j\|_{A_j,\infty,\Gamma}^2 |e_{ij}|^2 \lesssim \beta_i \quad (3.17)$$

where $e_i = [e_{i1} \ e_{i2}]^T$. This approach is beneficial in situations where the components of e_i are very different and there is a large difference between the $\|n_j\|_{A_j,\infty,\Gamma}^2$ with $j = 1$ and $j = 2$.

The Robust Finite Element Method. Find $u_h \in V_h$ such that

$$\boxed{\mathcal{A}_h^R(u_h, v) := \mathcal{A}^R(u_h, v) + s_h(u_h, v) = L(v) \quad \forall v \in V_h} \quad (3.18)$$

where

$$\mathcal{A}^R(v, w) = \mathcal{A}_1(v, w) + (n \cdot A \nabla v, B^{-1}(n \cdot A \nabla w))_\Gamma \quad (3.19)$$

$$- (n \cdot A \nabla v, B^{-1}(n \cdot A \nabla w) + (w - w_\Gamma))_\Gamma \quad (3.20)$$

$$- (B^{-1}(n \cdot A \nabla v) + (v - v_\Gamma), n \cdot A \nabla w)_\Gamma \quad (3.21)$$

$$+ (B^{-1}(n \cdot A \nabla v) + (v - v_\Gamma), \tau(B^{-1}(n \cdot A \nabla w) + (w - w_\Gamma)))_\Gamma. \quad (3.22)$$

It follows by the design of \mathcal{A}^R that for a sufficiently smooth exact solution $u \in \tilde{V}$ of the problem (2.26) there holds

$$\mathcal{A}(u, v) = \mathcal{A}^R(u, v) = L(v), \quad \forall v \in (V \cap H^2(\Omega_1 \cup \Omega_2 \cup \Gamma) + V_h). \quad (3.23)$$

As a consequence we immediately get the Galerkin orthogonality

Lemma 3.2 *Let $u \in \tilde{V}$ be the solution of (2.26) and $u_h \in V_h$ the solution of (3.18) then there holds*

$$\mathcal{A}^R(u - u_h, v) = s_h(u_h, v) \quad \forall v \in V_h. \quad (3.24)$$

Proof. The proof follows by combining (3.23) and (3.18). \square

4 Error Estimates

4.1 The Energy Norm

We introduce the energy norm

$$\|v\|_h^2 = \sum_{i=1}^2 \|\nabla v_i\|_{A_i, \Omega_i}^2 + h \|\nabla v_i\|_{A_i, \Gamma}^2 + \|v\|_{s_h}^2 + \|\nabla_\Gamma v_\Gamma\|_{A_\Gamma, \Gamma}^2 + \|v - v_\Gamma\|_{\tau, \Gamma}^2 \quad (4.1)$$

where $\|w\|_{\psi, \omega}^2 = \int_\omega \psi w^2$ is the ψ weighted L^2 norm over the set ω .

4.2 Interpolation Error Estimates

We begin by introducing the interpolation operators and derive the basic approximation error estimates. Then collecting the estimates we show an interpolation error estimate in the energy norm (4.1). Since the stabilization operator acts on the finite element solution outside its physical domain of definition, we must make sense of the solution it approximates also outside its physical domain of definition. We will show below how this can be done using extensions from the physical geometry.

The Scott-Zhang Interpolant. Given a mesh \mathcal{T}_h covering a domain O_h and the space of piecewise linear continuous finite elements W_h , the standard Scott-Zhang interpolation operator $\pi_{h, SZ} : H^1(\Omega_h) \rightarrow W_h$ satisfies the element wise estimate

$$\|v - \pi_{h, i, SZ} v\|_{H^m(T)} \lesssim h^{2-m} \|v\|_{H^2(\mathcal{N}(T))}, \quad m = 0, 1 \quad (4.2)$$

where $\mathcal{N}(T)$ is the set of all elements in $\mathcal{T}_{h, i}$ that share a node with T . Note also that the Scott-Zhang interpolant preserves homogeneous boundary conditions exactly. See [26] for further details.

Bulk Domain Fields. It is shown in [27, Section 2.3, Theorem 5] that there is an extension operator $E_i : H^s(\Omega_i) \rightarrow H^s(\mathbb{R}^d)$, not dependent on $s \geq 0$, which is stable in the sense that

$$\|E_i v_i\|_{H^s(\mathbb{R}^d)} \lesssim \|v_i\|_{H^s(\Omega_i)} \quad (4.3)$$

We define the interpolation operator $\pi_{h, i} : H^1(\Omega_i) \rightarrow V_{h, i}$ by

$$\pi_{h, i} v_i = \pi_{h, i, SZ} E_i v \quad (4.4)$$

where $\pi_{h, i, SZ} : H^1(O_{h, i}) \rightarrow V_{h, i}$ is the Scott-Zhang interpolant and we recall that $O_{h, i} = \cup_{T \in \mathcal{T}_{h, i}} T$ is the domain covered by $\mathcal{T}_{h, i}$. We then have the error estimate

$$\boxed{\|v_i - \pi_{h, i} v_i\|_{H^m(\Omega_i)} \lesssim h^{2-m} \|v_i\|_{H^2(\Omega_i)} \quad m = 0, 1} \quad (4.5)$$

Proof. Using the notation $\rho_i = v_i - \pi_{h,i}v_i$ we obtain

$$\|\rho_i\|_{H^m(\Omega_i)} \lesssim \|\rho_i\|_{H^m(O_{h,i})} \lesssim h^{2-m} \|E_i u_i\|_{H^2(O_{h,i})} \lesssim h^{2-m} \|u_i\|_{H^2(\Omega_i)}^2$$

where we used the fact that $\Omega_i \subset O_{h,i}$, the interpolation error estimate (4.2), and finally the stability (4.3) of the extension operator E_i . \square

Interface Field. Let $p_\Gamma : U_\delta(\Gamma) \rightarrow \Gamma$ be the closest point mapping from the tubular neighborhood $U_\delta(\Gamma) := \{x : \text{dist}(x, \Gamma) < \delta\}$ to Γ , which is well defined for all $\delta \in (0, \delta_0]$ for some $\delta_0 > 0$. Define the extension operator $E_\Gamma : L^2(\Gamma) \rightarrow L^2(U_\delta(\Gamma))$ by $E_\Gamma v = v \circ p_\Gamma$. Since Γ is smooth we have the stability estimate

$$\|E_\Gamma v_\Gamma\|_{H^s(U_\delta(\Gamma))} \lesssim \delta^{1/2} \|v_\Gamma\|_{H^s(\Gamma)}. \quad (4.6)$$

Observe also that since $n_\Gamma \cdot \nabla E_\Gamma v_\Gamma = 0$ by construction, and then assuming $s > 3/2$ in (4.6) we see that

$$s_{h,\Gamma}(E_\Gamma v_\Gamma, w) = 0, \forall w \in V_{h,\Gamma} + H^{\frac{3}{2}+\epsilon}(O_{h,\Gamma}). \quad (4.7)$$

To define the interpolant we first let

$$\mathcal{T}_{h,\delta,\Gamma} = \{T \in \mathcal{T}_{h,0} : T \cap U_\delta(\Gamma) \neq \emptyset\}, \quad O_{h,\delta,\Gamma} = \cup_{T \in \mathcal{T}_{h,\delta,\Gamma}} T \quad (4.8)$$

for $\delta \in (0, \delta_0/2]$. Then $O_{h,\Gamma} \subset O_{h,\delta,\Gamma}$ and there are $\delta, \delta' \in (0, \delta_0]$ such that $\delta \sim \delta' \sim h$ and

$$U_\delta(\Gamma) \subset O_{h,\delta,\Gamma} \subset U_{\delta'}(\Gamma) \subset U_{\delta_0}(\Gamma) \quad (4.9)$$

for all $h \in (0, h_0]$, with h_0 small enough. We let $V_{h,\delta,\Gamma} = V_{h,0}|_{O_{h,\delta,\Gamma}}$ and define $\pi_{h,\Gamma} : H^1(\Gamma) \rightarrow V_{h,\Gamma}$ by

$$\pi_{h,\Gamma} v_\Gamma = (\pi_{h,\delta,\Gamma,SZ} E_\Gamma v_\Gamma)|_{O_{h,\Gamma}} \quad (4.10)$$

where $\delta \sim h$ and $\pi_{h,\delta,\Gamma,SZ} : H^1(O_{h,\delta,\Gamma}) \rightarrow V_{h,\delta,\Gamma}$ is the Scott-Zhang interpolant. We have the error estimate

$$\|v - \pi_{h,\Gamma} v\|_{H^m(\Gamma)} \lesssim h^{2-m} \|v\|_{H^2(\Gamma)} \quad m = 0, 1 \quad (4.11)$$

Proof. Using the trace inequality

$$\|v\|_\Gamma^2 \lesssim \delta^{-1} \|v\|_{U_\delta(\Gamma)}^2 + \delta \|\nabla v\|_{U_\delta(\Gamma)}^2 \quad v \in H^1(U_\delta(\Gamma)) \quad (4.12)$$

where the hidden constant is independent of δ , we obtain

$$\begin{aligned} \|\nabla_\Gamma^m \rho\|_\Gamma^2 &\lesssim \delta^{-1} \|\nabla^m \rho\|_{U_\delta(\Gamma)}^2 + \delta \|\nabla^{m+1} \rho\|_{U_\delta(\Gamma)}^2 \\ &\lesssim \delta^{-1} \|\nabla^m \rho\|_{O_{h,\delta,\Gamma}}^2 + \delta \|\nabla^{m+1} \rho\|_{O_{h,\delta,\Gamma}}^2 \\ &\lesssim \delta^{-1} h^{2(2-m)} \|\nabla^2 E_\Gamma v\|_{O_{h,\delta,\Gamma}}^2 + \delta h^{2(1-m)} \|\nabla^2 E_\Gamma v\|_{O_{h,\delta,\Gamma}}^2 \\ &\lesssim \delta^{-1} h^{2(2-m)} \|\nabla^2 E_\Gamma v\|_{U_{\delta'}(\Gamma)}^2 + \delta h^{2(1-m)} \|\nabla^2 E_\Gamma v\|_{U_{\delta'}(\Gamma)}^2 \\ &\lesssim \delta^{-1} \delta' h^{2(2-m)} \|v\|_{H^2(\Gamma)}^2 + \delta \delta' h^{2(1-m)} \|v\|_{H^2(\Gamma)}^2 \\ &\lesssim h^{2(2-m)} \|v\|_{H^2(\Gamma)}^2 \end{aligned}$$

where we used (4.9), the interpolation error estimate (4.2), the stability (4.6) of the extension operator E_Γ , and the fact that $\delta \sim \delta' \sim h$. \square

We define the interpolation operator $\pi_h : V \rightarrow V_h$ as follows

$$\pi_h v = (\pi_{h,1} E_1 v_1, \pi_{h,2} E_2 v_2, \pi_{h,\Gamma} E_\Gamma v_\Gamma) \quad (4.13)$$

Lemma 4.1 *There is a constant not dependent on the matrix B , in the interface condition (2.3), such that*

$$\|v - \pi_h v\|_h \lesssim h \left(\sum_{i=1}^2 \|v_i\|_{H^2(\Omega_i)} + \|v_\Gamma\|_{H^2(\Gamma)} \right) \quad (4.14)$$

Proof. Let $v - \pi_h v = \rho$ be the interpolation error. Using the triangle inequality and (4.20),

$$\begin{aligned} \|\rho\|_h^2 &= \sum_{i=1}^2 \|\nabla \rho_i\|_{A_i, \Omega_i}^2 + h \|\nabla \rho_i\|_{A_i, \Gamma}^2 + \|\nabla_\Gamma \rho_\Gamma\|_{A_\Gamma, \Gamma}^2 + \|\rho_i - \rho_\Gamma\|_{\tau_i, \Gamma}^2 + \|\rho\|_{s_h}^2 \\ &\lesssim \sum_{i=1}^2 \|\nabla \rho_i\|_{\Omega_i}^2 + h \|\nabla \rho_i\|_\Gamma^2 + h^{-1} \|\rho_i\|_\Gamma^2 + \|\rho_i\|_{s_{h,i}}^2 \\ &\quad + \|\nabla_\Gamma \rho_\Gamma\|_\Gamma^2 + h^{-1} \|\rho_\Gamma\|_\Gamma^2 + \|\rho_\Gamma\|_{s_{h,\Gamma}}^2 \\ &\lesssim \sum_{i=1}^2 \left(\sum_{m=0}^2 h^{2(m-1)} \|\rho_i\|_{H^m(O_{h,i})}^2 \right) \\ &\quad + \|\nabla_\Gamma \rho_\Gamma\|_\Gamma^2 + h^{-1} \|\rho_\Gamma\|_\Gamma^2 + \left(\sum_{m=1}^2 h^{2(m-1)} \|\rho_i\|_{H^m(O_{h,\delta,\Gamma})}^2 \right) \\ &\lesssim \sum_{i=1}^2 h^2 \|E_i v_i\|_{H^2(O_{h,i})}^2 + h \|E_\Gamma v_\Gamma\|_{H^2(O_{h,\delta,\Gamma})}^2 \\ &\lesssim \sum_{i=1}^2 h^2 \|v_i\|_{H^2(\Omega_i)}^2 + h \delta' \|v_\Gamma\|_{H^2(\Gamma)}^2 \end{aligned}$$

with $\delta' \sim h$ and the desired estimate follows. Here we used the bounds

$$h \|\nabla \rho_i\|_\Gamma^2 + h^{-1} \|\rho_i\|_\Gamma^2 \lesssim \sum_{m=0}^2 h^{2(m-1)} \|\rho_i\|_{H^m(\Omega_i)}^2 \quad (4.15)$$

$$\|\rho_i\|_{s_{h,i}}^2 \lesssim \sum_{m=1}^2 h^{2(m-1)} \|\rho_i\|_{H^m(O_{h,i})}^2 \quad (4.16)$$

$$\|\rho_i\|_{s_{h,\Gamma}}^2 \lesssim \sum_{m=1}^2 h^{2(m-1)-1} \|\rho_i\|_{H^m(O_{h,\delta,\Gamma})}^2 \quad (4.17)$$

To prove (4.15) we employ the trace inequality

$$\|v\|_{\Gamma}^2 \lesssim \delta^{-1} \|v\|_{U_{\delta}(\Gamma) \cap \Omega_i}^2 + \delta \|\nabla v\|_{U_{\delta}(\Gamma) \cap \Omega_i}^2 \quad v \in H^1(\Omega_i)$$

with $\delta \sim h$, to estimate the interface terms involving ρ_i as follows

$$h \|\nabla \rho_i\|_{A_i, \Gamma}^2 \lesssim \|\rho\|_{H^1(U_{\delta}(\Gamma) \cap \Omega_i)}^2 + h^2 \|\rho\|_{H^2(U_{\delta}(\Gamma) \cap \Omega_i)}^2 \lesssim \|\rho\|_{H^1(O_{h,i})}^2 + h^2 \|\rho\|_{H^2(O_{h,i})}^2$$

and

$$h^{-1} \|\rho_i\|_{\Gamma}^2 \lesssim h^{-2} \|\rho_i\|_{U_{\delta}(\Gamma) \cap \Omega_i}^2 + \|\rho_i\|_{H^1(U_{\delta}(\Gamma) \cap \Omega_i)}^2 \lesssim h^{-2} \|\rho\|_{O_{h,i}}^2 + \|\rho\|_{H^1(O_{h,i})}^2$$

For (4.16) we apply the elementwise trace inequality

$$\|v\|_F^2 \lesssim h^{-1} \|v\|_T^2 + h \|\nabla v\|_T^2$$

which gives

$$\|\rho\|_{s_{h,i}}^2 \lesssim \sum_{m=1}^2 \sum_{T \in T_{h,i}} (\|\nabla \rho\|_T^2 + h \|\nabla^2 \rho\|_T^2) \lesssim \sum_{m=1}^2 h^{2(m-1)} \|v\|_{H^m(O_{h,i})}^2$$

In a similar way we prove (4.17), see [6] and [23] for details. \square

4.3 Continuity and Coercivity

We start with a lemma collecting some useful estimates for expressions involving the stabilization parameter τ and then we prove continuity and coercivity of the form A_h .

Lemma 4.2 *The following estimates related to the stabilization parameter τ hold*

$$\|B^{-1} \tau B^{-1} + B^{-1}\|_{L^{\infty}(\Gamma)} \leq \frac{h}{\beta} \quad (4.18)$$

$$\|(B^{-1} \tau - I) \tau^{-1/2}\|_{L^{\infty}(\Gamma)} \leq \left(\frac{h}{\beta}\right)^{1/2} \quad (4.19)$$

$$\|\tau\|_{L^{\infty}(\Gamma)} \leq \frac{\beta}{h} \quad (4.20)$$

Proof. First we recall that for any symmetric matrix D it holds

$$\|A\|_{\mathbb{R}^d} \lesssim \max_i |\gamma_i| \quad (4.21)$$

where γ_i are the eigenvalues of D . To prove (4.18) we write B in terms of its eigenvalues λ_i and eigenvectors e_i ,

$$B = \sum_{i=1}^2 \lambda_i e_i \otimes e_i \quad (4.22)$$

and using the definition (3.14) of τ we obtain the identity

$$B^{-1}\tau B^{-1} - B^{-1} = \sum_{i=1}^2 \left(\frac{\tau_i}{\lambda_i} - 1 \right) \frac{1}{\lambda_i} e_i \otimes e_i \quad (4.23)$$

Here we have the following estimate of the eigenvalues

$$\left| \left(\frac{\tau_i}{\lambda_i} - 1 \right) \frac{1}{\lambda_i} \right| = \left| \left(\frac{\beta}{\lambda_i h + \beta} - 1 \right) \frac{1}{\lambda_i} \right| = \frac{h}{\lambda_i h + \beta} \leq \frac{h}{\beta} \quad (4.24)$$

which in view of (4.21) completes the verification of (4.18). Next, for (4.19) we have

$$(B^{-1}\tau - I)\tau^{-1/2} = \sum_{i=1}^2 \left(\frac{\tau_i}{\lambda_i} - 1 \right) \frac{1}{\tau_i^{1/2}} e_i \otimes e_i \quad (4.25)$$

and

$$\begin{aligned} \left| \left(\frac{\tau_i}{\lambda_i} - 1 \right) \frac{1}{\tau_i^{1/2}} \right| &= \left| \left(\frac{\beta}{\lambda_i h + \beta} - 1 \right) \left(\frac{\lambda_i h + \beta}{\lambda_i \beta} \right)^{1/2} \right| \\ &= \frac{\lambda_i h}{\lambda_i h + \beta} \left(\frac{\lambda_i h + \beta}{\lambda_i \beta} \right)^{1/2} = \left(\frac{\lambda_i h}{\lambda_i h + \beta} \right)^{1/2} \left(\frac{h}{\beta} \right)^{1/2} \leq \left(\frac{h}{\beta} \right)^{1/2} \end{aligned} \quad (4.26)$$

which proves (4.19). The final bound (4.20) is a direct consequence of the definition of τ and the estimate

$$\frac{\lambda_i \beta}{\lambda_i h + \beta} \leq \frac{\lambda_i \beta}{\lambda_i h} \leq \frac{\beta}{h} \quad (4.27)$$

□

Lemma 4.3 *There is a constant independent of the eigenvalues of B , such that for all $v, w \in \tilde{V} + V_h$,*

$$\boxed{\mathcal{A}_h^R(v, w) \lesssim |||v|||_h |||w|||_h} \quad (4.28)$$

There is a constant independent of the eigenvalues of B , such that for all $v \in V_h$,

$$\boxed{|||v|||_h^2 \lesssim \mathcal{A}_h^R(v, v)} \quad (4.29)$$

Proof. (4.28). Starting from the definition (3.19), expanding the terms in \mathcal{A}^R ,

and using Cauchy-Schwarz we obtain

$$\mathcal{A}^R(v, w) = \sum_{i=1}^2 (A_i \nabla v_i, \nabla w_i)_{\Omega_i} + (A_\Gamma \nabla_\Gamma v_\Gamma, \nabla_\Gamma w_\Gamma)_\Gamma \quad (4.30)$$

$$\begin{aligned} &+ ((n \cdot A \nabla v), (B^{-1} \tau B^{-1} - B^{-1})(n \cdot A \nabla w))_\Gamma \\ &+ ((n \cdot A \nabla v), (B^{-1} \tau - I)(w - w_\Gamma))_\Gamma \\ &+ ((n \cdot A \nabla w), (B^{-1} \tau - I)(v - v_\Gamma))_\Gamma \\ &+ ((v - v_\Gamma), \tau(w - w_\Gamma))_\Gamma \\ &\leq \sum_{i=1}^2 \|\nabla v_i\|_{A_i, \Omega_i} \|\nabla w_i\|_{A_i, \Omega_i} + \|\nabla_\Gamma v_\Gamma\|_{A_\Gamma, \Gamma} \|\nabla_\Gamma w_\Gamma\|_{A_i, \Gamma} \quad (4.31) \\ &\quad + \|n \cdot A \nabla v\|_\Gamma \|B^{-1} \tau B^{-1} - B^{-1}\|_{L^\infty(\Gamma)} \|n \cdot A \nabla w\|_\Gamma \\ &\quad + \|n \cdot A \nabla v\|_\Gamma \|(B^{-1} \tau - I) \tau^{-1/2}\|_{L^\infty(\Gamma)} \|w - w_\Gamma\|_{\tau, \Gamma} \\ &\quad + \|n \cdot A \nabla w\|_\Gamma \|(B^{-1} \tau - I) \tau^{-1/2}\|_{L^\infty(\Gamma)} \|v - v_\Gamma\|_{\tau, \Gamma} \\ &\quad + \|v - v_\Gamma\|_{\tau, \Gamma} \|w - w_\Gamma\|_{\tau, \Gamma} \end{aligned}$$

$$= \star \quad (4.32)$$

Using the estimates (4.18)-(4.19) we obtain

$$\star \leq \sum_{i=1}^2 \|\nabla v_i\|_{A_i, \Omega_i} \|\nabla w_i\|_{A_i, \Omega_i} + \|\nabla_\Gamma v_\Gamma\|_{A_\Gamma, \Gamma} \|\nabla_\Gamma w_\Gamma\|_{A_\Gamma, \Gamma} \quad (4.33)$$

$$\begin{aligned} &+ \beta^{-1} h \|n \cdot A \nabla v\|_\Gamma \|n \cdot A \nabla w\|_\Gamma \\ &+ \beta^{-1/2} h^{1/2} \|n \cdot A \nabla v\|_\Gamma \|w - w_\Gamma\|_{\tau, \Gamma} \\ &+ \beta^{-1/2} h^{1/2} \|n \cdot A \nabla w\|_\Gamma \|v - v_\Gamma\|_{\tau, \Gamma} \\ &+ \|v - v_\Gamma\|_{\tau, \Gamma} \|w - w_\Gamma\|_{\tau, \Gamma} \\ &\leq \sum_{i=1}^2 \|\nabla v_i\|_{A_i, \Omega_i} \|\nabla w_i\|_{A_i, \Omega_i} + \|\nabla_\Gamma v_\Gamma\|_{A_\Gamma, \Gamma} \|\nabla_\Gamma w_\Gamma\|_{A_\Gamma, \Gamma} \quad (4.34) \end{aligned}$$

$$\begin{aligned} &+ (\beta^{-1} \|n\|_{A, \infty, \Gamma}^2) h^{1/2} \|\nabla v\|_{A, \Gamma} h^{1/2} \|\nabla w\|_\Gamma \\ &+ (\beta^{-1} \|n\|_{A, \infty, \Gamma})^{1/2} h^{1/2} \|\nabla v\|_{A, \Gamma} \|w - w_\Gamma\|_{\tau, \Gamma} \\ &+ (\beta^{-1} \|n\|_{A, \infty, \Gamma})^{1/2} h^{1/2} \|\nabla w\|_{A, \Gamma} \|v - v_\Gamma\|_{\tau, \Gamma} \\ &+ \|v - v_\Gamma\|_{\tau, \Gamma} \|w - w_\Gamma\|_{\tau, \Gamma} \\ &\lesssim \|v\|_h \|w\|_h \quad (4.35) \end{aligned}$$

where we used the bound $\beta^{-1} \|n\|_{A, \infty, \Gamma} \lesssim 1$, see (3.15). By the Cauchy-Schwarz inequality we have $s_h(v, w) \lesssim \|v\|_h \|w\|_h$.

(4.29). To prove the coercivity we have the identity

$$\mathcal{A}_h^R(v, v) = \sum_{i=1}^2 (A_i \nabla v_i, \nabla v_i)_{\Omega_i} + (A_\Gamma \nabla_\Gamma v_\Gamma, \nabla_\Gamma v_\Gamma)_\Gamma + s_h(v, v) \quad (4.36)$$

$$\begin{aligned} &+ ((n \cdot A \nabla v), (B^{-1} \tau B^{-1} - B^{-1})(n \cdot A \nabla v))_\Gamma \\ &+ 2((n \cdot A \nabla v), (B^{-1} \tau - I)(v - v_\Gamma))_\Gamma \\ &+ ((v - v_\Gamma), \tau(v - v_\Gamma))_\Gamma \\ &\geq \sum_{i=1}^2 \|\nabla v_i\|_{A_i, \Omega_i}^2 + \|\nabla_\Gamma v_\Gamma\|_{A_\Gamma, \Gamma}^2 + \|v\|_{s_h}^2 \\ &\quad - \beta^{-1} \|n\|_{A, \infty, \Gamma}^2 h \|\nabla v\|_{A, \Gamma}^2 \\ &\quad - 2(\beta^{-1} \|n\|_{A, \infty, \Gamma})^{1/2} h^{1/2} \|\nabla v\|_{A, \Gamma} \|v - v_\Gamma\|_{\tau, \Gamma} \\ &\quad + \|v - v_\Gamma\|_{\tau, \Gamma}^2 \end{aligned} \quad (4.37)$$

We conclude the argument as usual by estimating the negative terms as follows

$$\beta^{-1} \|n\|_{A, \Gamma}^2 h \|\nabla v\|_{A, \Gamma}^2 + 2(\beta^{-1} \|n\|_{A, \infty, \Gamma})^{1/2} h^{1/2} \|\nabla v\|_{A, \Gamma} \|v - v_\Gamma\|_{\tau, \Gamma} \quad (4.38)$$

$$\leq 3\beta^{-1} \|n\|_{A, \infty, \Gamma}^2 h \|\nabla v\|_{A, \Gamma}^2 + \frac{1}{2} \|v - v_\Gamma\|_{\tau, \Gamma}^2 \quad (4.39)$$

$$\leq 3\beta^{-1} \|n\|_{A, \infty, \Gamma}^2 C_I \left(\sum_{i=1}^2 \|\nabla v_i\|_{A_i, \Omega_i}^2 + \|v\|_{s_{h,i}}^2 \right) + \frac{1}{2} \|v - v_\Gamma\|_{\tau, \Gamma}^2 \quad (4.40)$$

$$\leq \frac{1}{2} \left(\sum_{i=1}^2 \|\nabla v_i\|_{A_i, \Omega_i}^2 + \|v\|_{s_{h,i}}^2 \right) + \frac{1}{2} \|v - v_\Gamma\|_{\tau, \Gamma}^2 \quad (4.41)$$

Here we used the inverse estimate

$$h \|\nabla v_i\|_{A_i, \Gamma}^2 \leq C_I (\|\nabla v_i\|_{A_i, \Omega_i}^2 + \|v\|_{s_{h,i}}^2) \quad (4.42)$$

which follows from the inverse bound

$$h \|\nabla v_i\|_{A_i, \Gamma \cap T}^2 \lesssim h \|\nabla v_i\|_{\Gamma \cap T}^2 \lesssim \|\nabla v_i\|_T^2 \lesssim \|\nabla v_i\|_{A_i, T}^2 \quad (4.43)$$

together with (3.8), and finally, we chose β large enough to guarantee that

$$3\beta^{-1} \|n\|_{A, \infty, \Gamma}^2 C_I \leq \frac{1}{2} \quad (4.44)$$

We conclude that

$$\mathcal{A}_h^R(v, v) \geq \frac{1}{2} \|v\|_h^2 \quad (4.45)$$

which completes the proof. \square

4.4 A priori Error Estimates

In this section we prove error estimates for the approximate solution u_h .

Theorem 4.1 *Let $u \in \tilde{V}$ be the solution of (2.26) and $u_h \in V_h$ be the solution of (3.18). Then there is a constant not dependent on the matrix B in the interface condition (2.3) such that*

$$\|u - u_h\|_h \lesssim h \left(\sum_{i=1}^2 \|f_i\|_{L^2(\Omega_i)} + \|f_\Gamma\|_{L^2(\Gamma)} \right) \quad (4.46)$$

Proof. First we decompose the error in the approximation error and the discrete error $u - u_h = u - \pi_h u + \pi_h u - u_h$ and note that by the triangle inequality

$$\|u - u_h\|_h \lesssim \|u - \pi_h u\|_h + \|\pi_h u - u_h\|_h. \quad (4.47)$$

The first term on the right hand side is bounded by (4.14). For the second term on the right hand side, using coercivity (4.29), Galerkin orthogonality (3.24), and continuity (4.28) we obtain

$$\|\pi_h u - u_h\|_h^2 \lesssim \mathcal{A}_h^R(\pi_h u - u_h, \pi_h u - u_h) \quad (4.48)$$

$$= \mathcal{A}^R(\pi_h u - u, \pi_h u - u_h) + s_h(\pi_h u, \pi_h u - u_h) \quad (4.49)$$

$$\lesssim \|\pi_h u - u\|_h \|\pi_h u - u_h\|_h. \quad (4.50)$$

In the last inequality we used that if $u^e := (Eu_1, Eu_2, E_\Gamma u_\Gamma) \in \tilde{V}$ then

$$s_h(\pi_h u, \pi_h u - u_h) = s_h(\pi_h u - u^e, \pi_h u - u_h) \lesssim \|\pi_h u - u\|_h \|\pi_h u - u_h\|_h. \quad (4.51)$$

Thus

$$\|u - u_h\|_h \lesssim \|u - \pi_h u\|_h \lesssim h \left(\sum_{i=1}^2 \|u_i\|_{H^2(\Omega_i)} + \|u_\Gamma\|_{H^2(\Gamma)} \right) \quad (4.52)$$

where we used the interpolation error estimate (4.14). To conclude we apply the regularity estimate (2.31). \square

Corollary 4.1 *Under the same assumptions as for Theorem 4.1 there holds*

$$s_h(u_h, u_h) \lesssim h \left(\sum_{i=1}^2 \|u_i\|_{H^2(\Omega_i)} + \|u_\Gamma\|_{H^2(\Gamma)} \right). \quad (4.53)$$

Proof. Using the triangle inequality we see that

$$\|u_h\|_{s_h} \leq \|\pi_h u\|_{s_h} + \|\pi_h u - u_h\|_{s_h} \quad (4.54)$$

The second term on the right hand side is bounded by the arguments of Theorem 4.1. For the first term on the right hand side recall that by the consistency properties of s_h and the construction of $\pi_h u$ there holds

$$s_h(\pi_h u, \pi_h u) = s_h(u^e - \pi_h u, u^e - \pi_h u) \quad (4.55)$$

We conclude the proof by applying (4.16)-(4.17). \square

The following error estimate in the L^2 -norm also holds

Theorem 4.2 *Let $u \in \tilde{V}$ be the solution of (2.26) and $u_h \in V_h$ be the solution of (3.18). Then there holds*

$$\|u_h - u\|_\Omega + \|u_{h,\Gamma} - u_\Gamma\|_\Gamma \lesssim h^2 \left(\sum_{i=1}^2 \|f_i\|_{L^2(\Omega_i)} + \|f_\Gamma\|_{L^2(\Gamma)} \right) \quad (4.56)$$

Proof. For $\psi_\Omega \in L^2(\Omega)$ and ψ_Γ , such that $\|\psi_\Omega\|_\Omega + \|\psi_\Gamma\|_\Gamma = 1$ let $\varphi := (\varphi_1, \varphi_2, \varphi_\Gamma) \in V$ be the weak solution to

$$\mathcal{A}(v, \varphi) = (\psi_\Omega, v)_\Omega + (\psi_\Gamma, v_\Gamma)_\Gamma. \quad (4.57)$$

Then by (2.31) we have

$$\|\varphi_1\|_{H^2(\Omega_1)} + \|\varphi_2\|_{H^2(\Omega_2)} + \|\varphi_\Gamma\|_{H^2(\Gamma)} \lesssim \|\psi_\Omega\|_\Omega + \|\psi_\Gamma\|_\Gamma \sim 1. \quad (4.58)$$

Let $e = (u_1 - u_{1,h}, u_2 - u_{2,h}, u_\Gamma - u_{\Gamma,h})$ and observe that using (3.23),

$$(\psi_\Omega, u_1 - u_{1,h})_{\Omega_1} + (\psi_\Omega, u_2 - u_{2,h})_{\Omega_2} + (\psi_\Gamma, u_\Gamma - u_{\Gamma,h})_\Gamma = \mathcal{A}(e, \varphi) = \mathcal{A}^R(e, \varphi). \quad (4.59)$$

Applying now the Galerkin orthogonality (3.24) we see that

$$\mathcal{A}^R(e, \varphi) = \mathcal{A}^R(e, \varphi - \pi_h \varphi) - s_h(e, \pi_h \varphi) = \mathcal{A}_h^R(e, \varphi - \pi_h \varphi). \quad (4.60)$$

By the continuity (4.28) we can bound the right hand side,

$$\mathcal{A}_h^R(e, \varphi - \pi_h \varphi) \lesssim \|e\|_h \|\varphi - \pi_h \varphi\|_h. \quad (4.61)$$

Then applying the approximation (4.14) and the regularity (4.58) we have

$$(\psi_\Omega, u_1 - u_{1,h})_{\Omega_1} + (\psi_\Omega, u_2 - u_{2,h})_{\Omega_2} + (\psi_\Gamma, u_\Gamma - u_{\Gamma,h})_\Gamma \lesssim h \|e\|_h. \quad (4.62)$$

We conclude by applying Theorem 4.1 in the right hand side and taking the supremum over the functions $(\psi_\Omega, \psi_\Gamma)$ in L^2 . \square

5 Numerical Examples

In this Section we illustrate the properties of the model and method by presenting some numerical results. In all examples we used $\beta = 10$ as a stabilization parameter.

5.1 Convergence and Robustness with Respect to Conditioning

We consider a simple example with known exact solution: the domain $(0, 1) \times (0, 1)$ is cut in half along a vertical line at $x = 1/2$. We take $A_1 = A_2 = A_\Gamma = I$ and choose a problem with exact solution $u = x(1 - x)y(1 - y)$. This solution corresponds (without coupling) to the source terms

$$f_i = 2x(1 - x) + 2y(1 - y)$$

Since the normal derivative of the exact solution is zero at $x = 1/2$, it does not contribute to the source term on the interface. We choose $f_\Gamma = 1/2$ corresponding to $u_\Gamma = y(1 - y)/4$, and thus $u_\Gamma = u$ at $x = 1/2$. We apply zero Dirichlet boundary conditions on u and on u_Γ (imposed on the boundary of the band of elements intersected by $(1/2, y)$). This is now the solution of (2.1)–(2.4) independent of B . A sample discrete solution is shown in Fig. 1 with u_Γ shown as a red line. We did not impose gradient jumps on the band (second term in $s_{h,\Gamma}$), normal stabilization proved sufficient in this case.

In Figs. 2–5 we show convergence for different choices of parameters in different norms. The method is completely robust with optimal convergence for all choices. In Fig. 6 we show the variation of the condition number (left) with respect to mesh refinement and choice of α . The condition number is $O(h^{-2})$ as expected and does not grow with α . We also show (right) the effect of using the non-robust method (3.5) which shows a linear dependence on α on a fixed mesh, while no such effect is present in the robust method. This robustness is important since α physically depends on the crack width [24] which is expected to be small.

5.2 Effect of Gradient Jump Stabilization

This example is taken from [24] with domain is $(0, 2) \times (0, 1)$ with Dirichlet data $u = 1$ at $x = 2$ and $u = 0$ at $x = 0$. Homogeneous Neumann data were applied at $y = 0$ and $y = 1$. Data were $f_i = f_\Gamma = 0$, $A_1 = A_2 = I$ and $A_\Gamma = a_\Gamma d I$ with $a_\Gamma = 2 \times 10^{-3}$ for $1/4 < y < 3/4$, $a_\Gamma = 1$ elsewhere, and with $d = 0.01$ (the thickness of the crack). Following [24] we then set $\alpha = 2a_\Gamma/d$.

To show the effect of stabilization, we chose to scale $s_{h,i}$ and $s_{h,\Gamma}$ by a parameter γ . We retained $\beta = 10$ and normal stabilization on the band. In Figs. 7–9 we show the effect of the parameter γ . When $\gamma = 0$ the jump in diffusion on the interface leads to slight instabilities at $y = 1/4$ and $y = 3/4$ which are visible to the eye. These are less pronounced for $\gamma = 10^{-2}$ and not significant for $\gamma = 1$. The overall solution agrees with that of [24].

5.3 Physical Effect of Crack Width

Finally, we show the effect of the crack width with respect to the solution. We used a domain $(0, 1) \times (0, 1)$ with a quarter circle crack, shown on the computational mesh in Fig. 10. The data were $A_1 = 5I$ (inside the circle)

$A_2 = I$ (outside the circle) and $a_\Gamma = 0.1$ with definitions as in Example 5.2. Dirichlet data $u = 1$ at $x = 1$ and $u = 0$ at $x = 0$ were used (also on the band) and homogeneous Neumann data on the remaining boundaries. In Figs. 11–13 we see the effect of decreasing the interface width by one order of magnitude between figures. The solution rapidly tends to a continuous state.

Acknowledgement. This research was supported in part by EPSRC, UK, Grant No. EP/P01576X/1, the Swedish Foundation for Strategic Research Grant No. AM13-0029, the Swedish Research Council Grants No. 2013-4708, 2017-03911, 2018-05262, and Swedish strategic research programme eSSSENCE.

References

- [1] P. Angot, F. Boyer, and F. Hubert. Asymptotic and numerical modelling of flows in fractured porous media. *M2AN Math. Model. Numer. Anal.*, 43(2):239–275, 2009.
- [2] P. F. Antonietti, C. Facciola, A. Russo, and M. Verani. Discontinuous Galerkin approximation of flows in fractured porous media on polytopic grids. *SIAM J. Sci. Comput.*, 41(1):A109–A138, 2019.
- [3] W. M. Boon, J. M. Nordbotten, and I. Yotov. Robust discretization of flow in fractured porous media. *SIAM J. Numer. Anal.*, 56(4):2203–2233, 2018.
- [4] E. Burman, S. Claus, P. Hansbo, M. G. Larson, and A. Massing. Cut-FEM: discretizing geometry and partial differential equations. *Internat. J. Numer. Methods Engrg.*, 104(7):472–501, 2015.
- [5] E. Burman and P. Hansbo. Fictitious domain finite element methods using cut elements: II. A stabilized Nitsche method. *Appl. Numer. Math.*, 62(4):328–341, 2012.
- [6] E. Burman, P. Hansbo, and M. G. Larson. A stabilized cut finite element method for partial differential equations on surfaces: the Laplace-Beltrami operator. *Comput. Methods Appl. Mech. Engrg.*, 285:188–207, 2015.
- [7] E. Burman, P. Hansbo, and M. G. Larson. A simple finite element method for elliptic bulk problems with embedded surfaces. *Comput. Geosci.*, 23(1):189–199, 2019.
- [8] E. Burman, P. Hansbo, M. G. Larson, and K. Larsson. Cut finite elements for convection in fractured domains. *Comput. & Fluids*, 179:726–734, 2019.
- [9] E. Burman, P. Hansbo, M. G. Larson, K. Larsson, and A. Massing. Finite element approximation of the Laplace-Beltrami operator on a surface with boundary. *Numer. Math.*, 141(1):141–172, 2019.

- [10] E. Burman, P. Hansbo, M. G. Larson, and D. Samvin. A cut finite element method for elliptic bulk problems with embedded surfaces. *GEM Int. J. Geomath.*, 10(1): 10, 2019.
- [11] E. Burman, P. Hansbo, M. G. Larson, and S. Zahedi. Cut finite element methods for coupled bulk-surface problems. *Numer. Math.*, 133(2):203–231, 2016.
- [12] D. Capatina, R. Luce, H. El-Otmany, and N. Barrau. Nitsche’s extended finite element method for a fracture model in porous media. *Appl. Anal.*, 95(10):2224–2242, 2016.
- [13] F. Chave, D. A. Di Pietro, and L. Formaggia. A hybrid high-order method for Darcy flows in fractured porous media. *SIAM J. Sci. Comput.*, 40(2):A1063–A1094, 2018.
- [14] A. Y. Chernyshenko and M. A. Olshanskii. An unfitted finite element method for the Darcy problem in a fracture network. *J. Comput. Appl. Math.* 366(1): 112424
- [15] A. Fumagalli and E. Keilegavlen. Dual virtual element method for discrete fractures networks. *SIAM J. Sci. Comput.*, 40(1):B228–B258, 2018.
- [16] S. Gross, M. A. Olshanskii, and A. Reusken. A trace finite element method for a class of coupled bulk-interface transport problems. *ESAIM Math. Model. Numer. Anal.*, 49(5):1303–1330, 2015.
- [17] A. Hansbo and P. Hansbo. An unfitted finite element method, based on Nitsche’s method, for elliptic interface problems. *Comput. Methods Appl. Mech. Engrg.*, 191(47-48):5537–5552, 2002.
- [18] A. Hansbo and P. Hansbo. A finite element method for the simulation of strong and weak discontinuities in solid mechanics. *Comput. Methods Appl. Mech. Engrg.*, 193(33-35):3523–3540, 2004.
- [19] A. Hansbo, P. Hansbo, and M. G. Larson. A finite element method on composite grids based on Nitsche’s method. *ESAIM: Math. Model. Numer. Anal.*, 37(3):495–514, 2003.
- [20] P. H. Hung and E. Sánchez-Palencia. Phénomènes de transmission à travers des couches minces de conductivité élevée. *J. Math. Anal. Appl.*, 47:284–309, 1974.
- [21] M. Juntunen and R. Stenberg. Nitsche’s method for general boundary conditions. *Math. Comp.*, 78(267):1353–1374, 2009.
- [22] M. Köppel, V. Martin, and J. E. Roberts. A stabilized lagrange multiplier finite-element method for flow in porous media with fractures. *GEM Int. J. Geomath.*, 10(1):7, Jan 2019.

- [23] M. G. Larson and S. Zahedi. Stabilization of high order cut finite element methods on surfaces. *arXiv e-prints*, page arXiv:1710.03343, Oct 2017. to appear in IMA J. Numer. Anal.
- [24] V. Martin, J. Jaffré, and J. E. Roberts. Modeling fractures and barriers as interfaces for flow in porous media. *SIAM J. Sci. Comput.*, 26(5):1667–1691, 2005.
- [25] M. A. Olshanskii and A. Reusken. Trace finite element methods for PDEs on surfaces. In *Geometrically unfitted finite element methods and applications*, volume 121 of *Lect. Notes Comput. Sci. Eng.*, pages 211–258. Springer, Cham, 2017.
- [26] L. R. Scott and S. Zhang. Finite element interpolation of nonsmooth functions satisfying boundary conditions. *Math. Comp.*, 54(190):483–493, 1990.
- [27] E. M. Stein. *Singular integrals and differentiability properties of functions*. Princeton Mathematical Series, No. 30. Princeton University Press, Princeton, N.J., 1970.
- [28] E. L. Yedeg, E. Wadbro, P. Hansbo, M. G. Larson, and M. Berggren. A Nitsche-type method for Helmholtz equation with an embedded acoustically permeable interface. *Comput. Methods Appl. Mech. Engrg.*, 304:479–500, 2016.

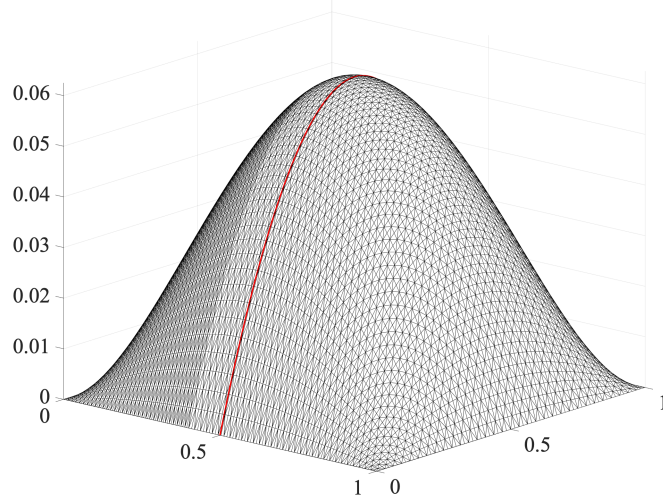


Figure 1: Elevation of the computed solution on a particular mesh (for $\alpha = 1$, $\xi = 1$).

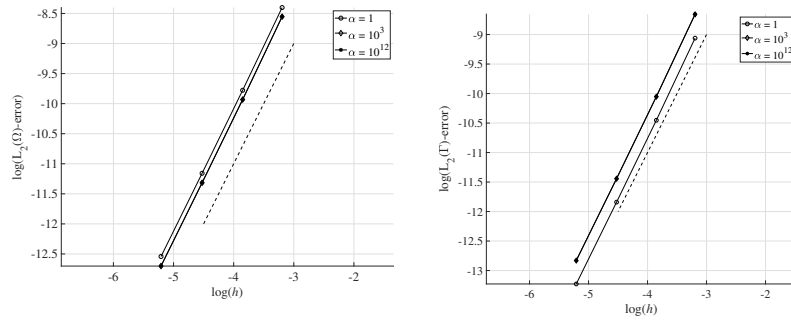


Figure 2: Convergence in $L_2(\Omega)$ and in $L_2(\Gamma)$ for varying α with $\xi = 1$. Dashed line has inclination 1:2.

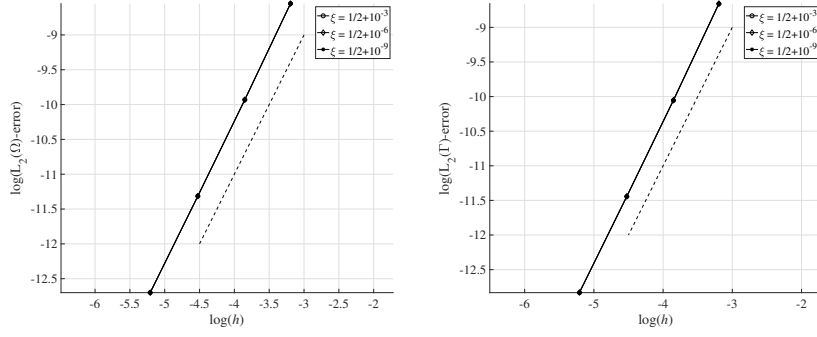


Figure 3: Convergence in $L_2(\Omega)$ and in $L_2(\Gamma)$ for varying ξ with $\alpha = 1$. Dashed line has inclination 1:2.

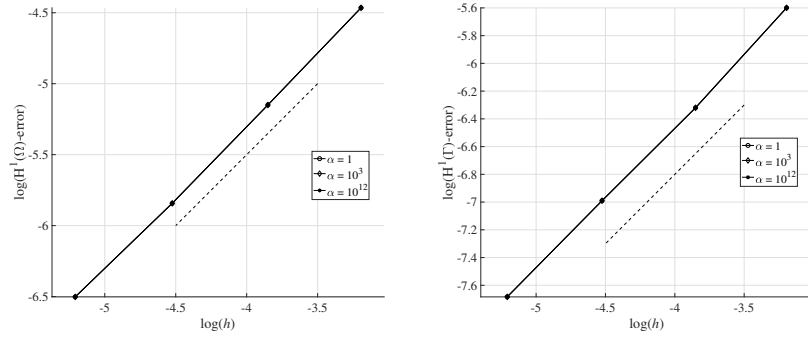


Figure 4: Convergence in $H^1(\Omega)$ and in $H^1(\Gamma)$ for varying α with $\xi = 1$. Dashed line has inclination 1:1.

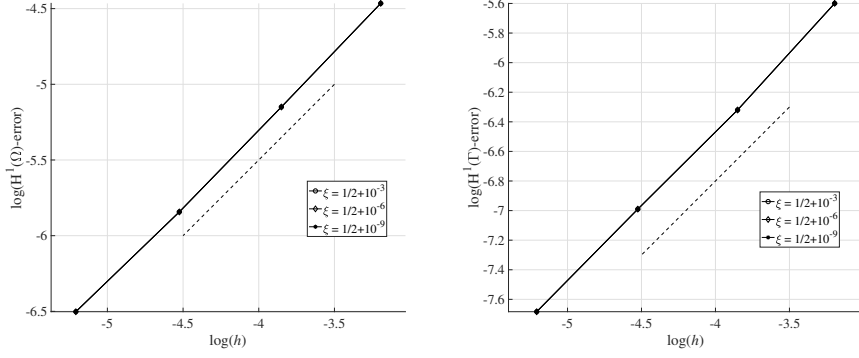


Figure 5: Convergence in $H^1(\Omega)$ and in $H^1(\Gamma)$ for varying ξ with $\alpha = 1$. Dashed line has inclination 1:1.

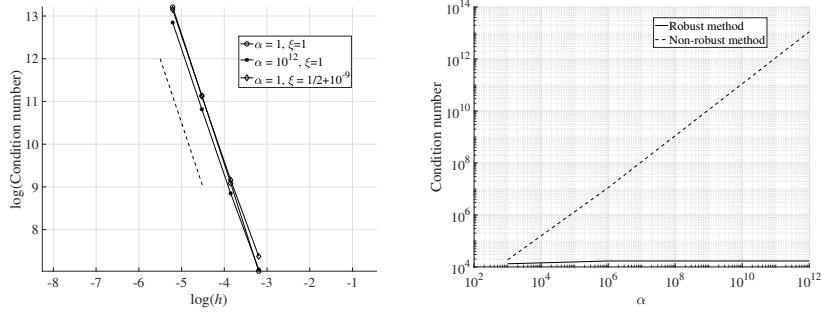


Figure 6: Left: Condition number as a function of meshsize. Dashed line has inclination 1:2. Right: condition numbers on a fixed mesh with varying α using the robust method (3.18) and the non-robust method (3.5).

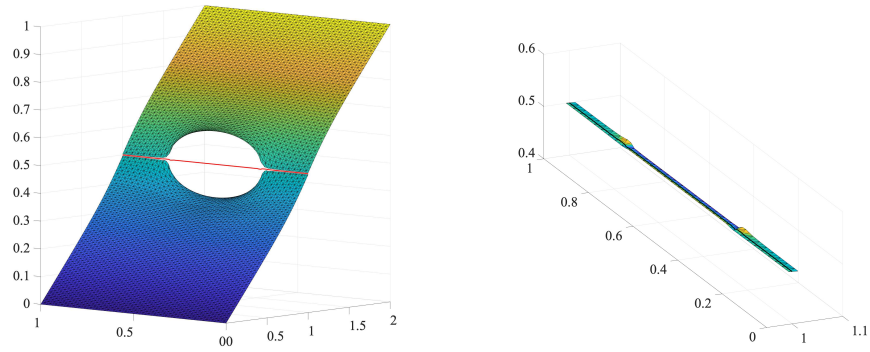


Figure 7: Elevation of the solution on Ω and the band containing Γ for $\gamma = 0$.

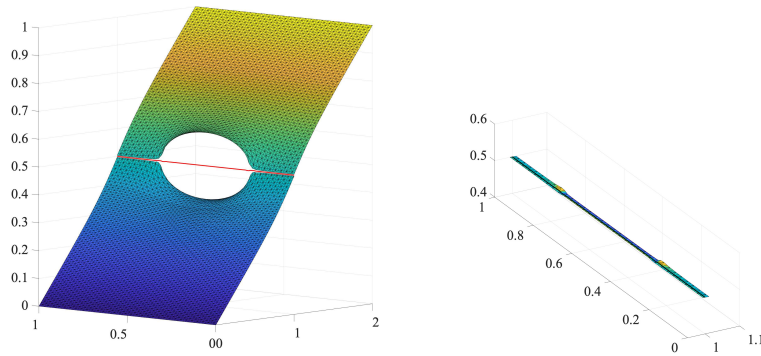


Figure 8: Elevation of the solution on Ω and the band containing Γ for $\gamma = 10^{-2}$.

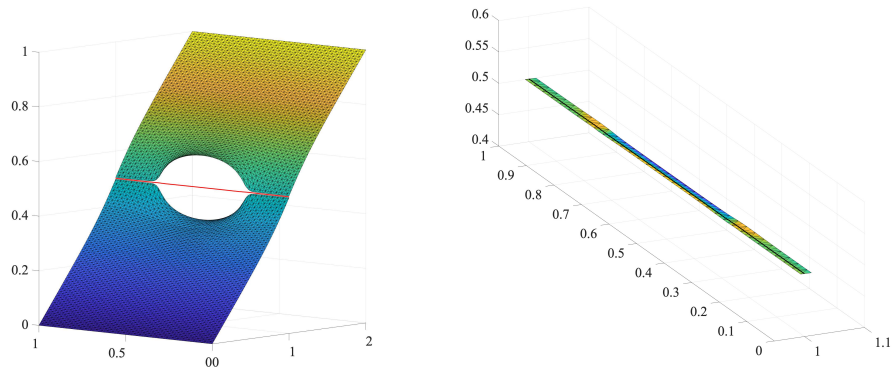


Figure 9: Elevation of the solution on Ω and the band containing Γ for $\gamma = 1$.

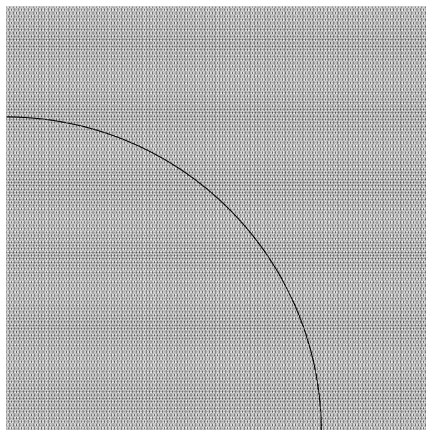


Figure 10: Computational mesh with interface indicated.

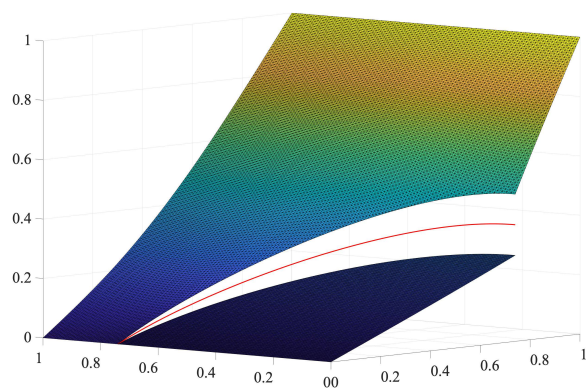


Figure 11: Elevation for $d = 10^{-2}$.

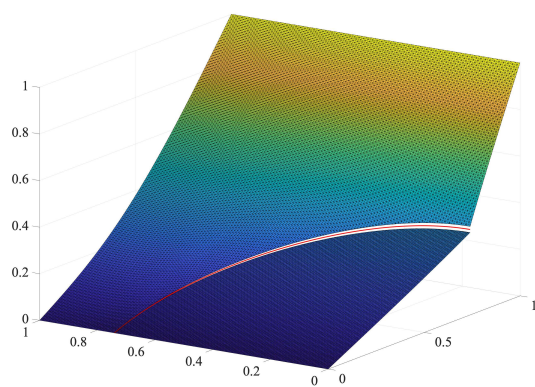


Figure 12: Elevation for $d = 10^{-3}$.

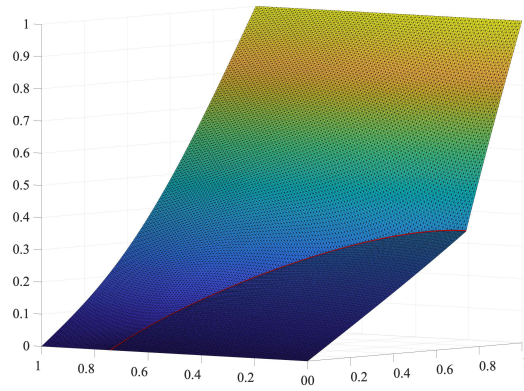


Figure 13: Elevation for $d = 10^{-4}$.